

Statistical Modeling of Fading and Diversity for Outdoor 60 GHz Channels ¹

Hong Zhang

Dept. of Electrical and Computer Engineering
University of California, Santa Barbara, USA
hongzhang@ece.ucsb.edu

Upamanyu Madhow

Dept. of Electrical and Computer Engineering
University of California, Santa Barbara, USA
madhow@ece.ucsb.edu

ABSTRACT

While there is significant ongoing effort in indoor applications of 60 GHz unlicensed wireless communication, the 60 GHz band also has significant potential in providing an easily deployable outdoor broadband infrastructure, using mesh networks with link ranges of the order of hundreds of meters. In this paper, we investigate the statistics of a typical lamppost-to-lamppost 60 GHz link by using ray tracing. Due to the directionality of the link, the multipath is sparse but strong, leading to significant fades that must be combated using multiple antennas. We show that the diversity provided by a 2×2 Multiple Input Multiple Output (MIMO) link with moderate antenna separation is sufficient for robust link performance. The two schemes we consider are transmit precoding along the dominant eigenmode (which requires channel state information at the transmitter) and the Alamouti space-time coding (which does not). We also show that the channel coefficients are well modeled as complex Gaussian with nonzero means, but the channel capacity is slightly overestimated by a Gaussian model whose correlations match those obtained from ray tracing.

Categories and Subject Descriptors

C.2.1 [Network Architecture and Design]: Wireless communication

General Terms

Performance

Keywords

MIMO, 60GHz, millimeter wave, outdoor channel modeling, channel capacity, diversity, fading

1. INTRODUCTION

While a great deal of industry attention is currently focused on indoor applications of unlicensed 60 GHz communication [1, 2], short-range outdoor communication in this

¹This research was supported in part by the National Science Foundation under grants CNS-0520335, ECS-0636621 and CNS-0832154.

Permission to make digital or hard copies of all or part of this work for personal or classroom use is granted without fee provided that copies are not made or distributed for profit or commercial advantage and that copies bear this notice and the full citation on the first page. To copy otherwise, to republish, to post on servers or to redistribute to lists, requires prior specific permission and/or a fee.

mmCom'10, September 24, 2010, Chicago, Illinois, USA.
Copyright 2010 ACM 978-1-4503-0142-8/10/09 ...\$10.00.

band with link ranges of the order of hundreds of meters also has significant potential in terms of providing an easily deployable broadband infrastructure. The higher free space loss (relative to lower carrier frequencies such as for the 2.4 or 5 GHz unlicensed bands) can be overcome by using highly directional transmit and receive antennas, which can be implemented using electronically steerable arrays. The characteristics of such highly directional links are fundamentally different from omnidirectional, or mildly directional, links at lower carrier frequencies. It is therefore critical to develop statistical models for such links, since existing link models developed for lower carrier frequencies do not apply. In particular, the multipath is sparse, but individual reflected paths can be strong, and the overall channel gain can fluctuate significantly with small changes in the propagation geometry. Thus, despite having a strong line of sight (LoS) component, we cannot obtain a robust link using a single directive antenna (which can be realized, for example, using an electronically steerable array of $\lambda/2$ spaced elements) at each end. In this paper, we employ ray tracing to investigate the statistics of a 2×2 MIMO link, comprising two directive antennas at each end, spaced at multiple wavelengths to provide diversity. The propagation geometry corresponds to a lamppost-based deployment with a nominal range of 200 meters.

The work reported here builds on our previous work in the same setting [3], where we introduced a 6-ray model, including the LoS path, the ground reflection, and single and double reflections from the walls on either side of the street. The new contributions in this paper are as follows. We first investigate the antenna spacing required to provide robust performance. Since our goal is to find the minimum spacing (i.e., the smallest form factor), we focus on diversity rather than spatial multiplexing gains, since the latter fluctuate wildly for the antenna spacings we are interested in here. In particular, we evaluate the performance of *dominant eigenmode transmission* (with transmit precoding along the stronger of the two eigenmodes) and *Alamouti space-time coding*, relative to a benchmark LoS link with the same range. In addition, we investigate the statistics of the individual channel coefficients, and show that, despite the small number of multipath components, they are well modeled as complex Gaussian with nonzero means (where the nonzero means are due to the strong LoS component). For moderate antenna spacings (large enough to provide “sufficient diversity”), capacity computed with the Gaussian model, setting the correlation coefficients to be those obtained from ray tracing, provide a

good (but slightly optimistic) approximation to the capacity obtained by ray tracing.

Related Work: Most measurement campaigns and channel modeling efforts in the millimeter (mm) wave band have focused on indoor settings [4, 5]. For outdoor city street type settings like those considered here, prior work has mainly been restricted to lower carrier frequencies such as 5 GHz [6]. Interference analysis [7] and MAC design [8] for mm wave mesh networks have yielded encouraging results on spatial reuse and inter-node coordination despite the deafness caused by highly directional links. However, these network-level studies employed idealized LoS link models, while our focus here is link-level robustness.

2. SYSTEM DESCRIPTION

2.1 Environment Geometry

As depicted in Figure 1, we consider an mm wave outdoor link with nodes deployed on the top of lamp-posts, which are typically lower than the surrounding buildings. The city street on which the lampposts are deployed is assumed to be straight between the two nodes considered. The buildings on both sides of the street are assumed to form a continuum. Intuitively, this is expected to be a worst-case scenario, because gaps between the buildings lead to fewer reflected paths, and hence less channel variations.

Our aim is to provide a robust link in a network system under a range of variations in the propagation geometry, so that our performance statistics are compiled for the following *canonical randomized geometry*. We model the lamppost heights at each end to be uniformly distributed over the interval $[2m, 5m]$, and the distances from the walls at each end of the street as uniform over $[2m, 14m]$. The heights and wall distances are independent random variables.

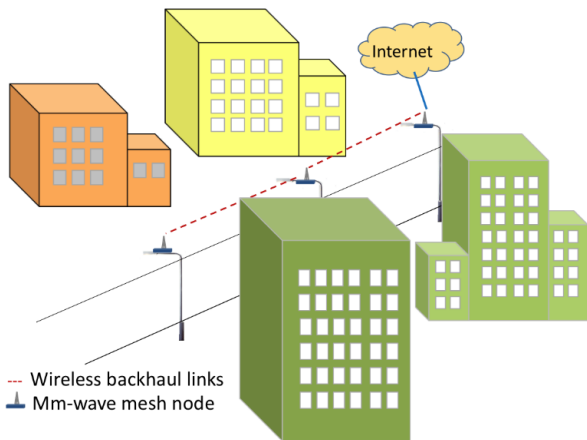


Figure 1: Millimeter wave nodes deployed on lamp-posts along a city street.

2.2 Nominal Link Parameters

We consider a 2 Gbps QPSK link over a distance of 200 meters with 1.5 GHz bandwidth, transmit and receive antenna directivities of 20 dBi each. For an uncoded Bit Error Rate (BER) of 10^{-9} , the target SNR is 15 dB. For a receiver noise figure of 5 dB and a link margin of 10 dB, the required transmit power is about 24 dBm. Since our goal is to investigate the effect of multipath propagation, we ignore rain attenuation, which of course can be significant at mm wave frequencies [9].

Antenna: We assume transmit and receive antennas with 10° horizontal beamwidth and 30° vertical beamwidth. In order to consider a realistic pattern, we employ the pattern generated by the open-slot antenna designed by our collaborators [10].

2.3 MIMO System

As shown in [3], a lamppost-based deployment can incur severe fading despite having a strong LoS component. We therefore consider a 2×2 MIMO system, as in [3]. The narrowband MIMO channel model is given by

$$\mathbf{y} = \mathbf{H}\mathbf{x} + \mathbf{w} \quad (1)$$

where (1) \mathbf{y} denotes the 2×1 received signal vector, (2) \mathbf{H} represents the 2×2 channel matrix, (3) \mathbf{x} denotes the 2×1 transmitted signal vector and (4) \mathbf{w} denotes 2×1 additive complex white Gaussian noise with covariance matrix $\mathbf{C}_w = \begin{bmatrix} N_1 & 0 \\ 0 & N_2 \end{bmatrix}$. It is useful to write the channel matrix as

$$\mathbf{H} = \mathbf{H}_{LOS} + \mathbf{H}_{Ref} \quad (2)$$

where \mathbf{H}_{LOS} and \mathbf{H}_{Ref} are contributions from the LoS path and reflected paths. The elements in H_{Ref} are given by $H_{Ref}(m, n) = \sum_i^{N_{Ref}} h_{Ref_i}(m, n)$, where N_{Ref} denotes the number of reflected paths and $h_{Ref_i}(m, n)$ is given by:

$$\frac{\lambda}{4\pi d_{Ref_i}(m, n)} G_{t_i}(m, n) G_{r_i}(m, n) e^{-j \frac{2\pi}{\lambda} d_{Ref_i}(m, n)} \quad (3)$$

Likewise, the element in H_{LOS} denoted by $H_{LOS}(m, n)$ is given by:

$$\frac{\lambda}{4\pi d_{LOS}(m, n)} G_{t_{LOS}}(m, n) G_{r_{LOS}}(m, n) e^{-j \frac{2\pi}{\lambda} d_{LOS}(m, n)} \quad (4)$$

where λ is the wavelength of the 60 GHz band; d_{LOS} and d_{Ref_i} denote the propagation path lengths of the LoS and reflected paths respectively; $G_{t_{LOS}}$, G_{t_i} , $G_{r_{LOS}}$, and G_{r_i} are the voltage gains of the transmit and receive antennas for the LoS path and the i th reflected path respectively.

Before proceeding further, we summarize some relevant observations from our previous paper [3]. As a result of the narrow horizontal beamwidths at the transmitter and receiver, wall reflections experiencing more than two bounces can be neglected, since they fall outside the beamwidth at the ranges of interest. This leads to a 6 ray model, including the LoS path, the ground reflection, and the one-bounce and two-bounce wall reflections from either side of the street. The fading from this model is severe enough that a Single Input Single Output (SISO) system is not robust. However, capacity computations in [3] show that using standard space-time communication techniques, robust performance can be obtained with a 2×2 MIMO link, where the two antennas at a given node being located along the body diagonal of a cube, with dimensions of the order of several wavelengths. A key goal in this paper is to understand the statistics of the performance obtained in such a 2×2 MIMO system.

3. CHANNEL EIGENMODE STATISTICS

For large enough antenna separation, spatial multiplexing can be obtained even in LoS environments, as demonstrated in [11]. However, at the moderate spacings of interest to us here, the 2×2 MIMO channel is typically rank deficient, since the scattering provided by the sparse multipath channel is not ‘‘rich enough.’’ We quantify the effect of antenna separation on the channel condition number (defined

shortly), and then focus on the performance statistics for Alamouti space-time coding, whose performance also serves as a lower bound for that of dominant eigenmode transmission. Our performance benchmark is an ideal LoS single input single output (SISO) link.

3.1 Channel Condition Number

We define the channel condition number as $\kappa = \lambda_{max}/\lambda_{min}$, where λ_{max} and λ_{min} correspond to the eigenvalues of the Wishart matrix $\mathbf{H}\mathbf{H}^H$. Note that κ is the ratio of the power gains seen by the two eigenmodes. Table 1 shows the mean condition number (averaged over 14000 realizations of the canonical randomized geometry) as a function of antenna separation. Note that the mean decreases from 28.8 dB to 5.7 dB as the antenna separation increases from 0.5λ to 10λ , but that the decrease is not monotonic because of the inherent correlations due to sparse multipath. Also, taking κ bigger than 10 dB as our definition of poor conditioning, we find that the channel is ill conditioned with a probability of about 50% even at relatively large antenna separations. Thus, while there may well be performance gains from an adaptive strategy that trades off diversity and multiplexing depending on the channel condition number, we focus in this paper on determining how predictable a performance can be obtained by pure diversity strategies.

Table 1: Statistics of the channel condition number as a function of antenna separation.

	0.5λ	5λ	10λ	20λ	30λ	40λ
$\bar{\kappa}(dB)$	28.8	10.5	5.72	6.36	8.32	8.22
$P(\kappa > 10dB)$	0.99	0.76	0.21	0.40	0.54	0.49

3.2 Statistics of the Dominant Eigenmode

The dominant eigenvalue of $\mathbf{H}\mathbf{H}^H$ can be expressed as:

$$\lambda_{max} = \frac{a+d}{2} + \frac{\sqrt{4bc + (a-d)^2}}{2} \quad (5)$$

where a, b, c, d are defined in the Equation 6.

$$A = \mathbf{H}\mathbf{H}^H = \begin{bmatrix} h_{11}h_{11}^* + h_{12}h_{12}^* & h_{11}h_{21}^* + h_{12}h_{22}^* \\ h_{21}h_{11}^* + h_{22}h_{12}^* & h_{21}h_{21}^* + h_{22}h_{22}^* \end{bmatrix} = \begin{bmatrix} a & b \\ c & d \end{bmatrix} \quad (6)$$

This can be lower bounded as follows:

$$\lambda_{max} \geq \frac{a+d}{2} = \frac{\text{trace}(A)}{2} = \gamma_{Alamouti} \quad (7)$$

where the lower bound on the right-hand side, $\frac{\text{trace}(A)}{2}$, can be recognized to be the normalized gain for Alamouti space-time coding scheme ($\gamma_{Alamouti}$) serving as the lower bound for the dominant eigenvalues. This normalized gain ($\gamma_{Alamouti} = 0.5 \times (h_{11}h_{11}^* + h_{12}h_{12}^* + h_{21}h_{21}^* + h_{22}h_{22}^*)$) is the average power of the channel matrix. Thus, we could obtain a diversity order of 4 if these four channels fade independently (which they do not for our sparse multipath channel).

In order to compare the Alamouti scheme (and by extension, the dominant eigenmode transmission scheme for which it provides a lower bound in performance) against the idealized LoS benchmark, we define the normalized free space gain:

$$\gamma_{free} = G_t G_r \left(\frac{\lambda}{4\pi d} \right)^2 \quad (8)$$

where G_t and G_r denote the transmit and receive antenna power gains, and d denotes the transmission range. The outage probability is therefore given by $P\{\gamma_{Alamouti} < \alpha\gamma_{free}\}$,

as a function of $\alpha \leq 1$, corresponding to the link margin allocated for fading. That is, $-10 \log_{10} \alpha$ is the link margin in dB; for example, 3 dB corresponds to $\alpha = \frac{1}{2}$. As showed in Figure 2, we note that a link margin of 5 dB is enough to reduce the outage probability to 2% for antenna separations bigger than 5λ .

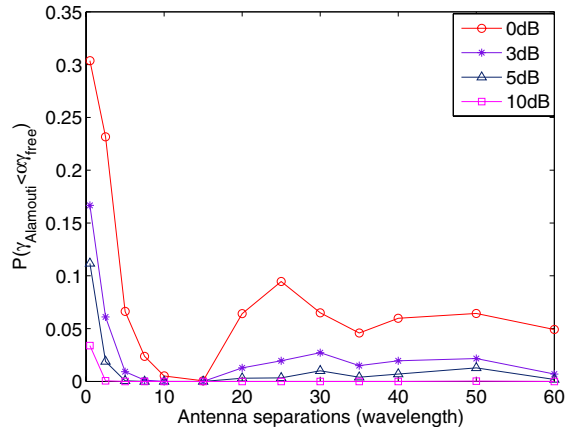


Figure 2: Outage probability for Alamouti scheme (which is an upper bound on outage probability for dominant eigenmode transmission).

4. GAUSSIAN FIT FOR CHANNEL COEFFICIENTS

We now explore the distribution of the channel coefficients in the 2×2 MIMO matrix. For simplicity, we normalize the channel matrix in Equation 2 with the LoS path component $H_{LOS}(1,1)$. Since $H_{LOS}(1,1)$ approx $H_{LOS}(2,2)$, the normalized channel matrix is given by:

$$\tilde{H} = \tilde{H}_{LOS} + \tilde{H}_{Ref} = \begin{bmatrix} 1 & e^{-j\theta_{12}} \\ e^{-j\theta_{21}} & 1 \end{bmatrix} + \tilde{H}_{Ref} \quad (9)$$

where $\theta_{12} = \frac{2\pi}{\lambda}(d_{LOS}(1,2) - d_{LOS}(1,1))$ and $\theta_{21} = \frac{2\pi}{\lambda}(d_{LOS}(2,1) - d_{LOS}(1,1))$. The elements of \tilde{H}_{Ref} can be expressed as:

$$\tilde{H}_{Ref}(m,n) = \sum_i^{N_{Ref}} \alpha_i(m,n) e^{-j\phi_i(m,n)} \quad (10)$$

where the amplitude $\alpha_i(m,n) = \frac{d_{LOS}(1,1)G_{t_i}(m,n)G_{r_i}(m,n)}{d_{Ref_i}(m,n)G_{t_{LOS}}(1,1)G_{r_{LOS}}(1,1)}$ and the phase term $\phi_i(m,n) = \frac{2\pi}{\lambda}(d_{Ref_i}(m,n) - d_{LOS}(1,1))$.

Figure 3 shows the histograms of the normalized channel coefficients in \tilde{H}_{Ref} . We see that these coefficients are well modeled as zero mean Gaussian random variables. Once the LoS components \tilde{H}_{LOS} are included, the channel coefficients in the overall channel matrix \tilde{H} can be modeled as nonzero mean Gaussian distributions.

$$r_{vec(\tilde{H})vec(\tilde{H})^H} = r_{vec(\tilde{H}_{Ref})vec(\tilde{H}_{Ref})^H} = \begin{bmatrix} 1 & r_1 & t_1 & s_1 \\ r_1^* & 1 & s_2 & t_2 \\ t_1^* & s_2^* & 1 & r_2 \\ s_1^* & t_2^* & r_2^* & 1 \end{bmatrix} \quad (11)$$

The correlation matrix of $vec(\tilde{H})$ is given by Equation 11, where r_i denotes correlation between receiving antennas and t_i represents correlation between transmitting antennas.

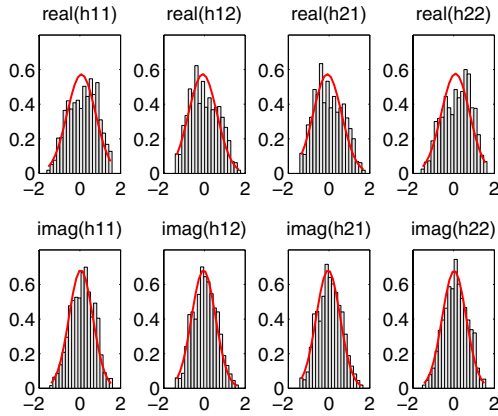


Figure 3: Histograms of the reflected channel coefficients.

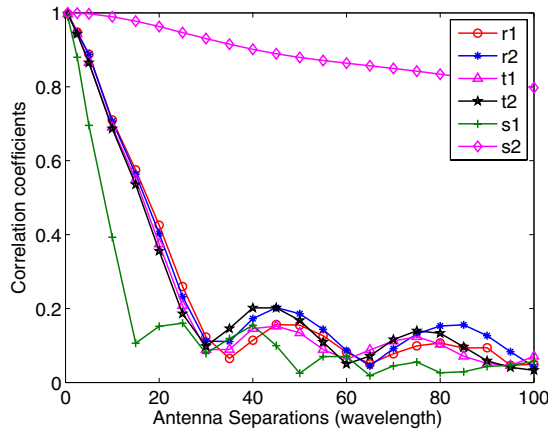


Figure 4: Correlation coefficients between channel coefficients.

s_i is the correlation between diagonal terms of the channel coefficients and also called diagonal correlation. The correlation coefficients are plotted in Figure 4, which shows that the channel matrix is highly correlated when antenna separations are smaller than 10λ . As the antenna separation increases beyond 25λ , all the correlation coefficients are around or below 0.2 except the correlation between h_{12} and h_{21} , which is still higher than 0.8 even when the antenna separation increases upto 100λ . This is because each reflected path bouncing from the same scatterer from transmitter 1 to receiver 2 is parallel with the corresponding path from transmitter 2 to receiver 1 for our setting (the correlation could be reduced by small random changes in the alignment, but a high correlation is actually a worst-case scenario which we would wish to be robust against).

The mean and variance of the power gain (7) for the Alamouti scheme can be computed as a function of the preceding correlations. These results are omitted due to lack of space, but they show that the mean is relatively insensitive to antenna spacing, while the bulk of the contribution to the variance comes from correlations between cross terms in the channel matrix, which can be reduced by increasing the

antenna spacing to about 25λ . However, as we note later, robust performance can be obtained at significantly smaller spacings (e.g., 5λ).

5. MIMO CAPACITY SIMULATIONS

We compare channel capacity estimates based on a Gaussian model (with correlation coefficients computed with ray tracing) with estimates directly obtained by averaging the mutual information for channel matrices generated by ray tracing. We also compare with the capacity for i.i.d. Rayleigh fading and Rician fading. *We only consider dominant eigenmode transmission or Alamouti in these capacity plots.*

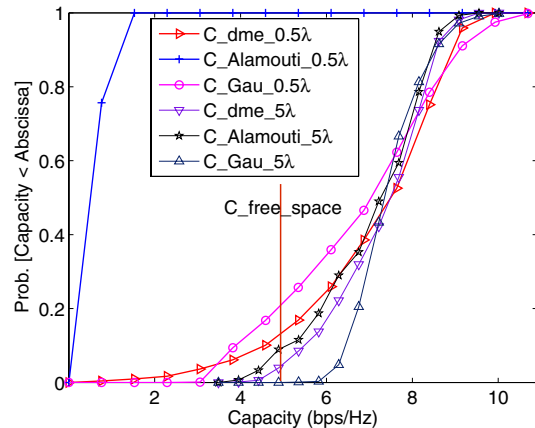


Figure 5: CDFs of capacity of dominant eigenmode transmission (ray tracing and correlated Gaussian for dominant eigenmode transmission (dme), ray tracing for Alamouti).

5.1 Comparison with correlated Gaussian model

Figure 5 shows that the CDF of the capacity obtained from the correlated Gaussian model roughly matches that obtained directly from ray tracing for dominant eigenmode transmission. Figure 6 shows that the 10% outage capacity between the ray tracing capacity and the capacity obtained from correlated Gaussian channel exhibits a small gap less than 0.5 bps if the antenna separation is equal to or larger than 5λ .

We also plot the ray-tracing capacity corresponding to the Alamouti scheme (recall that this serves as a lower bound for the capacity with dominant eigenmode transmission, in addition to being of interest in its own right). Figure 5 shows that the capacity for the Alamouti scheme is close to the capacity for the dominant eigenmode transmission for antenna separations of 5λ or more, but the gap is much larger at small separations such as 0.5λ . This is because the second term in (5) for dominant eigenmode transmission (which does not appear in the power gain for the Alamouti scheme), becomes significant at smaller separations: this term is large when the correlation between the channel coefficients is large.

5.2 Comparison with i.i.d. Rayleigh fading

In Figure 7, we compare the CDFs of the channel capacity using dominant eigenmode transmission for our ray tracing model with those for i.i.d. Rayleigh and Rician fading channels with the same powers. We set the Rician K factor to the average ratio of the Line of Sight signal power and the overall scattered signal power obtained in our ray tracing

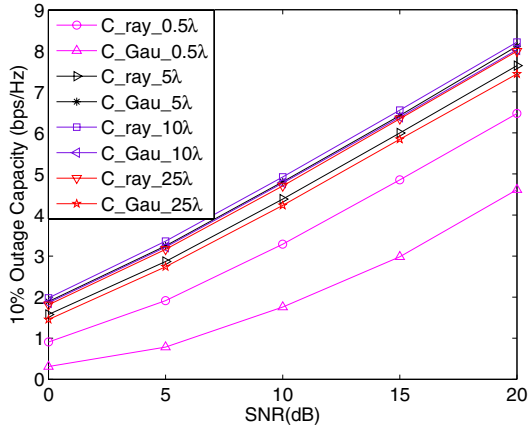


Figure 6: Outage capacity of dominant eigenmode transmission (ray tracing versus Gaussian fit) with different antenna separations.

simulations; this equals 1.2 in our simulations. For the 10% outage capacities indicated in the plot, the six-ray channel gives a lower capacity than the Rician fading channel (1.83 bps on average) even if the antenna separation is increased to 25λ . When there is no LoS path, we see that the corresponding 5-ray model yields lower 10% outage capacity (1.7 bps on average) than a corresponding i.i.d. Rayleigh fading model. Thus, the smaller level of averaging in our sparse multipath model does lead to significant loss of performance even for a pure diversity strategy. The performance gap would be even larger if spatial multiplexing were considered, since our channel is frequently rank deficient, where the i.i.d. Rayleigh or Rician channels have full rank with a high probability.

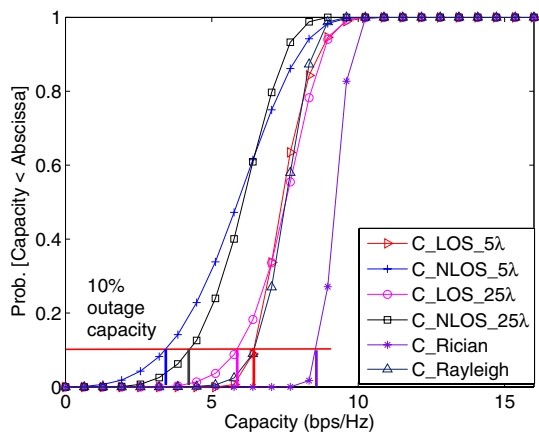


Figure 7: CDFs of channel capacity: comparison of sparse multipath channel with i.i.d. Rayleigh or Rician fading.

6. CONCLUSION

For the lamppost-based outdoor setting considered in this paper, moderate antenna separations (5λ or more) are found to be sufficient to provide diversity against the significant fades resulting from the sparse but strong multipath asso-

ciated with highly directional links. We cannot, however, count on spatial multiplexing gains unless the separations are much larger than those considered here, since the 2×2 channel matrix is often rank deficient. We find that i.i.d. Rayleigh or Rician fading models with similar parameters significantly overestimate performance. A Gaussian approximation to the channel coefficients (with nonzero means due to the strong LoS component), with correlation coefficients estimated from ray tracing, does provide a rough estimate of channel capacity, but is slightly off in estimating outage capacity. Since we do not have analytical rules of thumb for the channel correlations as a function of system parameters, the utility of the Gaussian model in quantifying performance measures such as outage is unclear: ray tracing must be used in any case to estimate the correlations between the channel coefficients, so that directly computing capacity based on the channel matrices generated by ray tracing is quite computationally efficient by comparison.

From a practical point of view, our results imply that transceiver design for nodes with compact form factor should focus on diversity strategies such as dominant eigenmode transmission or Alamouti space-time coding. Larger nodes, however, can provide robust spatial multiplexing [11]. Important topics for further research include measurement-based validation of our models, hardware realizations of nodes that can provide both diversity and beamsteering capabilities, and network level design.

7. REFERENCES

- [1] <http://wirelessgigabitalliance.org>, January 2010.
- [2] J. Gilbert, C. Doan, S. Emami, and C. B. Shung, "A 4-Gbps uncompressed wireless HD A/V transceiver chipset," *IEEE Micro*, vol. 28, no. 2, March 2008.
- [3] H. Zhang, S. Venkateswaran and U. Madhow, "Channel modeling and MIMO capacity for outdoor millimeter wave links," in *Proc. IEEE WCNC 2010*, Apr. 2010.
- [4] H. Xu, V. Kukshya, and T. S. Rappaport, "Spatial and temporal characteristics of 60-GHz indoor channels," *IEEE J. Select. Areas Commun.*, vol. 20, no. 3, 2002.
- [5] S. Geng, J. Kivinen, X. Zhao, and P. Vainikainen, "Millimeter-Wave Propagation Channel Characterization for Short-Range Wireless Communications." *IEEE Vehicular Tech.*, vol. 58, no. 1, pp. 3-13, Jan. 2009.
- [6] R. Mazar, A. Bronshtern, and I.-Tai Lu, "Theoretical analysis of UHF propagation in a city street modeled as a random multislit waveguide," *IEEE Trans. Antennas Propagat.*, vol. 46, no. 6, pp. 864-871, Jun. 1998.
- [7] R. Mudumbai, S. Singh, and U. Madhow, "Medium access control for 60 GHz outdoor mesh networks with highly directional links," in *Proc. IEEE INFOCOM 2009, Mini Conference*, Apr. 2009, pp. 2871-2875.
- [8] S. Singh, F. Ziliotto, U. Madhow, E. M. Belding, and M. Rodwell, "Blockage and Directivity in 60 GHz WPA Networks: From Cross-Layer Model to Multihop MAC Design," *IEEE JSAC, Special Issue on Realizing Gbps Wireless Personal Area Networks*, 2009.
- [9] V. Kvicera and M. Grabner, "Rain Attenuation at 58 GHz: Prediction versus Long-Term Trial Results," in *Proc. EURASIP J. Wireless Commun. Netw.* 2007
- [10] M. Seo, B. Ananthasubramaniam, M. Rodwell, and U. Madhow, "Millimeterwave imaging sensor nets: a scalable 60-GHz wireless sensor network," *2007 IEEE MTT-S Int. Microwave Symp. Dig.*, June 2007.
- [11] C. Sheldon, M. Seo, E. Torkildson, M. Rodwell, and U. Madhow, "Four-Channel Spatial Multiplexing Over a Millimeter-Wave Line-of-Sight Link," *MTTS International Microwave Symposium*, Boston, Massachusetts, June 2009.